

Hydrogenation of Borollide–Tantalum Complexes: Low-Valent Intermediates and the Effect of Exocyclic Substituents

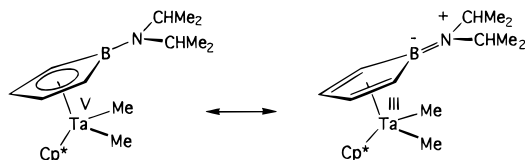
Caroline M. Kowal and Guillermo C. Bazan*

Department of Chemistry
University of Rochester
Rochester, New York, 14627

Received June 10, 1996

Dianionic borollide ligands^{1,2} have found recent applications in metallocene and low-valent chemistry.³ This ligand type provides a change in the ligand–metal relationship without deviating too far from well-characterized cyclopentadienyl (Cp) systems. Borollide metallocenes not only provide innovative catalytic possibilities in terms of polymerization and heterolytic bond activation reactions but also serve as new templates for the study of basic metal-mediated transformations.

Thus far, only the borollide ring containing diisopropylamine substitution at boron has been used in metallocene-like chemistry.⁴ Strong B–N π orbital overlap is observed together with a strong contribution from a diolefin/reduced-metal resonance structure. In Cp*[C₄H₄BN(CHMe₂)₂][TaMe₂] (**1**), the Ta–B distance is 2.70(1) Å while the B–N distance is 1.44(1) Å.⁵ Therefore, these are “ambivalent” molecules which need to be represented as resonance hybrids between two canonical forms.



Protonation at nitrogen interrupts the B–N π orbital overlap, and as a result, the metal–boron distances contract, favoring the high-valent resonance description. Therefore, it may be possible to modulate the electron density at the metal center by choice of exocyclic substituent. In this paper, we report the synthesis of Cp*[C₄H₄BMe][TaMe₂] (**2**), a high-valent methyl borollide metallocene and our studies on the mechanism of hydrogenation of both **1** and **2**, which show a reductive elimination oxidative addition pathway.

The reaction of excess AlMe₃ with Cp*[C₄H₄BMe][TaMeCl]^{3d} affords **2** in 70–80% yield. An X-ray diffraction study of **2** (Scheme 1) reveals a metallocene-like environment with a Ta–B distance (2.56(2) Å) which is closer to that of [Cp*[C₄H₄BNH-

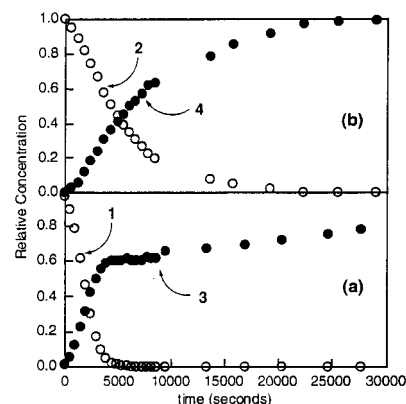


Figure 1. Reaction progress (at 620 Torr, 25 °C and with 5 equiv of PMe₃) for the conversion of (a) **1** to **3** and (b) **2** to **4**.

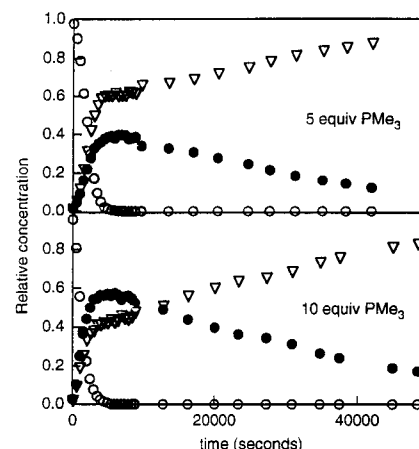


Figure 2. Comparison of reaction progress for conversion of **1** to **3** for 5 vs 10 equiv of PMe₃ at 25 °C under 620 Torr of H₂. (Open circles are for **1**, solid circles for **3**, and triangles for **5**.)

(CHMe₂)₂][TaMe₂][B(C₆F₅)₄] (2.537(6) Å) than that of neutral **1**. Methyl substitution therefore favors the high oxidation state description.⁶

Hydrogenation reactions of both **1** and **2** are much faster (over 3 orders of magnitude at 1 atm of H₂) than similar reactions of the isoelectronic group 4 metallocenes (*i.e.*, Cp*₂ZrMe₂).⁷ Phosphine traps the products as the monophosphine adducts Cp*[C₄H₄BN(CHMe₂)₂][Ta(H)₂PMe₃] (**3**) and Cp*[C₄H₄BMe][Ta(H)₂PMe₃] (**4**) (Scheme 1). The rates for disappearance of both **1** and **2** are linearly dependent on the concentration of starting material and hydrogen pressure, at least in the range of pressures accessible for these studies. The relative concentrations of **1** and **2** together with their corresponding products as a function of time and under identical conditions are shown in Figure 1. Note that **1** reacts faster with H₂ than **2** and that **4** appears at a faster rate than **3**. Addition of excess PMe₃ inhibits product formation but does not affect the rates at which **1** and **2** are consumed. The two slopes of Figure 1a indicate that at least two independent reactions take place to generate **3** and imply the presence of an intermediate or side product. Fast production of **3** occurs while **1** is present in solution followed by a slower process at longer reaction times.

(6) A decrease in π orbital overlap between boron and its substituent results in a stronger boron–metal interaction and high oxidation state characteristics. For a detailed discussion, see: (a) Herberich, G. E.; Englert, U.; Hostalek, M.; Laven, R. *Chem. Ber.* **1991**, *124*, 17. (b) Ashe, A. J., III; Kampf, J. W.; Müller, C.; Schneider, M. *Organometallics* **1996**, *15*, 387.

(7) (a) Miller, F. D.; Sanner, R. D. *Organometallics* **1988**, *7*, 818. (b) Lin, Z.; Marks, T. J. *J. Am. Chem. Soc.* **1987**, *109*, 7979. (c) Jordan, R. F.; Bajgur, C. S.; Dasher, W. E.; Rheingold, A. L. *Organometallics* **1987**, *6*, 1041.

(1) (a) Noth, H.; Schmidt, M. *Angew. Chem., Int. Ed. Engl.* **1996**, *35*, 292. (b) For a survey of new ligands in metallocene complexes, see: Bochmann, M. *J. Chem. Soc., Dalton Trans.* **1996**, 255.

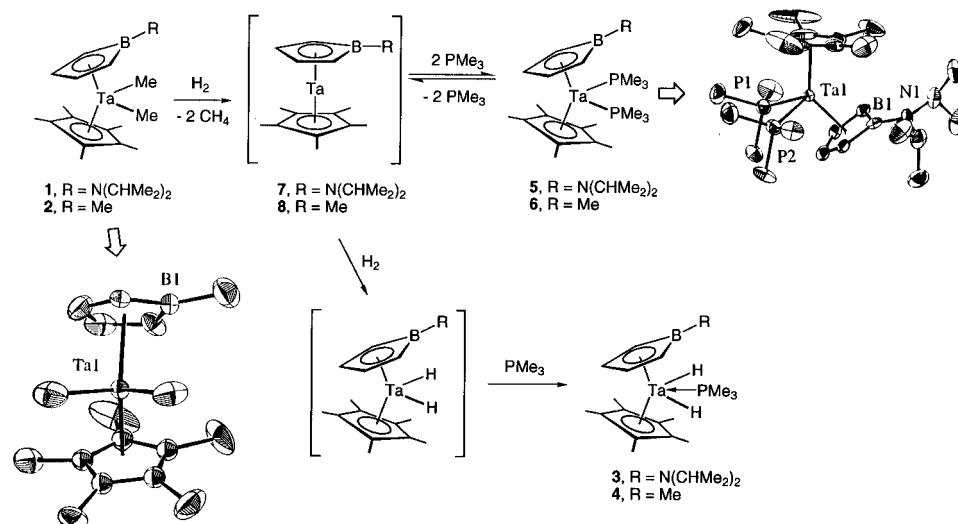
(2) For a recent review, see: Herberich, G. E. In *Comprehensive Organometallic Chemistry II*; Abel, E. W.; Stone, F. G. A., Wilkinson, G., Eds.; Pergamon Press: Oxford, 1995; Vol. 1, p 197.

(3) (a) Vanadium and niobium: Herberich, G. E.; Hausmann, I.; Klaff, N. *Angew. Chem., Int. Ed. Engl.* **1989**, *28*, 319. (b) Zirconium and hafnium metallocenes: Quan, R. W.; Bazan, G. C.; Kiely, A. F.; Schaeffer, W. P.; Bercaw, J. E. *J. Am. Chem. Soc.* **1994**, *116*, 4489. (c) Tantalum metallocenes: Bazan, G. C.; Rodriguez, G. *Polyhedron* **1995**, *14*, 93–102. (d) Bazan, G. C.; Donnelly, S. J.; Rodriguez, G. *J. Am. Chem. Soc.* **1995**, *117*, 2671–2672.

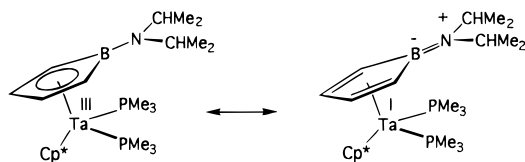
(4) Herberich, G. E.; Hostalek, M.; Laven, R.; Boese, R. *Angew. Chem., Int. Ed. Engl.* **1990**, *23*, 317.

(5) N–B distances cover a wide range, depending on the extent of π orbital overlap. For a N–B distance of 1.557(8) Å, see: Ansoorge, A.; Brauer, D. J.; Bürger, H.; Dorrenbach, F.; Hagen, T.; Pawelke, G.; Weuter, W. *J. Organomet. Chem.* **1991**, *407*, 283. A short distance of 1.371(8) Å was observed: Engelhardt, L. M.; Jacobsen, G. E.; Junk, P. C.; Raston, C. L.; White, A. H. *J. Chem. Soc., Chem. Commun.* **1990**, 89.

Scheme 1



New organometallic species were detected during our spectroscopic studies. They are characterized by one Cp*, one borollide, and two PMe₃ ligands and are assigned as Cp*-[C₄H₄BN(CHMe₂)₂]Ta(PMe₃)₂ (**5**) in the reactions with **1** and Cp*-[C₄H₄BMe]Ta(PMe₃)₂ (**6**) when **2** is used. As shown in Figure 2, addition of phosphine increases the relative concentration of **5**, and this is the only product in neat PMe₃-d₉ (there is no evidence of **3** in this solvent, even after 1 month). Pure **5**-d₁₈ formed in this way can be converted quantitatively to **3** by redissolving into C₆D₆ and reacting with phosphine and H₂. The structure of **5**-d₁₈, shown in Scheme 1, confirms our assignment. There is a short B–N distance (1.44(1) Å), and the Ta–B distance is longer (2.757(4) Å) than that measured in **1**, perhaps as a result of the more crowded ligand environment. These metrical parameters suggest contributions from resonance structures involving Ta(III) and Ta(I) oxidation states.



With these observations, we propose that formation of **3** from **1** proceeds *via* the sequence of reactions shown in Scheme 1. Reaction of **1** with H₂ generates 2 equiv of CH₄ and “Cp*-[C₄H₄BN(CHMe₂)₂]Ta” (**7**). Two reaction paths are available to **7**. The first is oxidative addition of H₂ and PMe₃ coordination to give **3** and accounts for the fast growth of **3** observed at earlier reaction times (*i.e.*, the first 5000 s in Figure 1a). Alternatively, **7** binds phosphine to form **5**. That PMe₃ must then dissociate from **5** before H₂ addition can take place accounts for the slower process at longer reaction times. Excess

phosphine retards the formation of **3** by accelerating the formation of **5** relative to oxidative addition of H₂. It is not clear at the present time if H₂ can react with a monophosphine adduct. Nonetheless, we are certain that a reductive elimination/oxidative addition cycle is required to form **3** from **1**.

Scheme 1 also applies to **2**. However, it is interesting that the more electron rich **1** reacts faster than **2** (Figure 1). This observation disfavors a σ bond metathesis step as the rate-determining step. Furthermore, **7** has a more pronounced tendency than Cp*-[C₄H₄BMe]Ta (**8**) to bind PMe₃, relative to reaction with H₂. Boron substituents therefore affect the relative rates of these elementary chemical steps.

These findings are significant within metallocene chemistry. Alkyl substituents on the borollide ring enforce high oxidation state characteristics to the metal and, as shown by **5**, low-valent tantalum–aminoborollide complexes also display “ambivalent” characteristics. Reductive elimination/oxidative addition cycles, such as those observed in the formation of **3** and **4** from **1** and **2**, have rarely been observed in early transition metal chemistry. This observation raises the intriguing possibility that similar mechanisms may be operating in hydrogenation reactions of group 4 metallocenes.

Acknowledgment. The authors gratefully acknowledge the Petroleum Research Fund and Exxon Chemical Company for financial support and the help of Dr. Brian P. Cleary and Mr. Scott J. Donnelly in the early stages of the project. We also thank Professors William D. Jones, W. Donald Cotter, and John E. Bercaw for stimulating discussions. G.C.B. is an Alfred P. Sloan Research Fellow and a Camille and Henry Dreyfus Teacher-Scholar.

Supporting Information Available: Experimental details for hydrogenation reactions, synthesis, and X-ray crystallographic determination of **2** and **5** (59 pages). See any current masthead page for ordering and Internet access instructions.

JA961934J